Ni-Al_2O_3/Ni-Foam Catalyst with Enhanced Heat Transfer for Hydrogenation of CO_2 to Methane

Yakun Li, Qiaofei Zhang, Ruijuan Chai, Guofeng Zhao, Ye Liu, and Yong Lu
Shanghai Key Laboratory of Green Chemistry and Chemical Processes, School of Chemistry and Molecular Engineering, East China Normal University, Shanghai 200062, China

Fahai Cao
College of Chemical Engineering, East China University of Science and Technology, Shanghai 200237, China

DOI 10.1002/aic.14935
Published online July 26, 2015 in Wiley Online Library (wileyonlinelibrary.com)

Monolithic Ni-Al_2O_3/Ni-foam catalyst is developed by modified wet chemical etching of Ni-foam, being highly active/selective and stable in strongly exothermic CO_2 methanation process. The as-prepared catalysts are characterized by x-ray diffraction scanning electron microscopy, inductively coupled plasma atomic emission spectrometry, and H_2-temperature programmed reduction-mass spectrometry. The results indicate that modified wet chemical etching method is working efficiently for one-step creating and firmly embedding NiO-Al_2O_3 composite catalyst layer (~2 μm) into the Ni-foam struts. High CO_2 conversion of 90% and high CH_4 selectivity of >99.9% can be obtained and maintained for a feed of H_2/CO_2 (molar ratio of 4/1) at 320°C and 0.1 MPa with a gas hourly space velocity of 5000 h^{-1}, throughout entire 1200 h test over 10.2 mL such monolithic catalysts. Computational fluid dynamics calculation and experimental measurement consistently confirm a dramatic reduction of "hotspot" temperature due to enhanced heat transfer. *AIChE J*, 61: 4323–4331, 2015
Keywords: heterogeneous catalysis, structured catalyst, methanation, foam, computational fluid dynamics simulation

Introduction

Concerns about the global warming and climate change caused by the greenhouse effects warrant increasing attention for the CO_2 emission control.[1–4] In principle, three methods including reducing the consumption of fossil fuels, carbon capture and sequestration, and conversion of CO_2 into fuels and chemicals can be adopted to reduce the CO_2 emission. As a renewable route, converting CO_2 into fuels and chemicals (e.g., methanol) has been attracting fast growing attention especially via photoelectrocatalysis and electrocatalysis.[1,5–11] In spite of ongoing efforts to significantly extend our understanding of the fundamental science concerning these new approaches, there is still a long way to go to reach practical use, as the process efficiency is unacceptably low from the economic view point. In contrast, the hydrogenation of CO_2 to methane (or CO_2 methanation), also known as Sabatier reaction, is highly efficient and most promising in case hydrogen is available or is obtainable from renewables.[12,13] Actually, it is an indispensable reaction in the production of substitute natural gas (SNG) from syngas consisting of H_2, CO, and CO_2 in varying ratios, which can be generated from various carbon sources such as biomass. Notably, the overall thermal efficiency for biomass and coal to SNG can reach 62–65%, which is much higher than coal to oil (40–50%) and coal to electricity (36–38%).[14,15] Moreover, such synthetic methane can be injected into the already existing gas distribution infrastructure (e.g., pipelines).[14]

Although the CO_2 methanation is thermodynamically favorable ($\Delta G_{25°C} = -113.5$ kJ mol^{-1}), it suffers from significant kinetic limitations because CO_2 is awfully stable and the reaction involves an eight-electron reduction.[3] To promote the transformation of CO_2, high operation temperature (250–450°C) is usually needed. Conversely, this reaction is highly exothermic ($\Delta H_{25°C} = -165$ kJ mol^{-1}) with adiabatic temperature rise of ~600°C in the first methanation reactor, therefore, inducing unexpected hotspots in the reactor bed, which not only is a main cause for catalyst deactivation but is also dangerous in industrial applications. Up to date, most attention has been focused on development of the efficient and stable catalysts almost with no shooting a glance at heat-transfer solutions. Many catalysts, including non-noble metal oxides (e.g., Ni/MCM-41,[16] Fe/SiO_2,[17] and Co/SiO_2[17]), and noble metal oxides (e.g., Ru/TiO_2,[18] Rh/γ-Al_2O_3,[19] and Pd/γ-Al_2O_3[19]), have been extensively investigated in CO_2 hydrogenation to methane. Regardless of their cost-efficiency and durability requirement in practical applications, in case of packed bed (PB) reactor, several reactors connected in series with sufficient intermediate gas cooling or product gas recycling have to be required to move away the reaction heat. This operation mode is high energy consumption and low efficiency, by nature, undoubtedly due to poor thermal

Additional Supporting Information may be found in the online version of this article.

Correspondence concerning this article should be addressed to Y. Lu at ylu@chem.ecnu.edu.cn.

conductivity of the traditional oxides-supported catalysts.[20,21] Although thinner reactor tube PB with smaller particle size could achieve more uniform temperature distribution, the larger pressure drop will lead to extra problems such as stability, safety, and cost. Fluidized bed enjoys improved heat-transfer efficiency inside the reactor but suffers some disadvantages such as low efficiency, low durability, and high cost.[22] Therefore, it is highly desirable to develop a novel catalyst system with a combination of excellent activity, small pressure drop, high thermal conductivity, and structural robustness.

Recently, microstructured catalyst has been attracting growing interests in the heterogeneous catalysis due to the improved hydrodynamics in combination with enhanced heat/mass transfer.[23–25] And a great deal of effort has been expended on developing novel structured catalysts with enhanced heat-transfer characteristics for applications in highly endothermic/exothermic reactions, such as metal microfibrous entrapped catalysts for the dry reforming of methane[26,27] and Fischer–Tropsch synthesis,[28,29] macroscopic stainless-steel-fiber@HZSM-5 core-shell catalysts for the methanol-to-propylene (MTP),[30,31] nanoporous-gold/Al-fiber catalysts obtained by galvanic deposition method for the methanol selective oxidation to methyl formate,[32,33] and Au/Ni-fiber[34,35] and Ag/Cu-fiber catalysts[36,37] for the gas-phase oxidation of alcohols. Notably, metallic foams also provide attractive opportunities as substrates for microstructured catalysts especially for the strongly exothermic or endothermic reaction processes, because of their advantages of favorable mass/heat transfer, desired mechanical robustness, high surface area to volume, and low pressure drop.[38,39] Despite these outstanding features, their practical application still appears challenging on efficiently endowing the metal-foams high catalytic performance comparable to the traditional catalysts. Directly using metal foams as active components (e.g., Cu and Ni) and catalyst coatings are explored extensively, but the former provides low activity due to deficient surface active sites while homogeneous coating of foam is usually difficult because of its cellular geometry, fragility during the reaction as well as binder contamination.[40–42]

In this study, we discover a hierarchical three-dimensional pore Ni-Al_2O_3/Ni-foam composite catalyst engineered from microscales to macroscales, where the uniform porous Ni-Al_2O_3 catalyst layer embedded onto the Ni-foam struts has a NiO/Al_2O_3 mass ratio of ~3.4. This new approach provides a combination of enhanced heat transfer, desired mechanical robustness, and excellent catalytic performance and reaction stability in the strongly exothermic hydrogenation of CO_2 to methane.

Experimental

Catalyst preparation

The metal foam catalyst of Ni-Al_2O_3/Ni-foam was fabricated on macroscale using modified wet chemical etching method followed by thermal treatment activation.[43–48] Ni foam (100 pores per inch) chips (diameter of 16 mm, equal to the reactor inner diameter) were prepared by laser cutting and then directly immersed into a chemical etching solution, heated to 65°C and held at that temperature for 2 h. The chemical etching solution was composed of 1.0 mmol L^{-1} sodium dodecyl sulphate (SDS, $C_{12}H_{25}$-OSO_3Na), 0.2 mol L^{-1} acetic-acid (CH_3COOH) and 0.3 mol L^{-1} aluminum nitrate ($Al(NO_3)_3{\cdot}9H_2O$), where the chemicals were all purchased from Sinopharm Chemical Reagent Co. Ltd. and directly used without further treatment. The optimal dosage of chemical etching solution is 2000 mL solution per 100 g Ni-foam. After chemical etching, the resulting metal-foam chips were thoroughly washed using distilled water and dried overnight at 100°C, followed by calcining in air at 550°C for 2 h to obtain Ni-Al_2O_3/Ni-foam catalyst.

For comparison, a Ni/Al_2O_3 catalyst was prepared by incipiently impregnating the support of γ-Al_2O_3 (Alfa Aesar) with an aqueous solution of using $Ni(NO_3)_2{\cdot}6H_2O$ as precursor to NiO loading of 15%, followed by calcining in air at 550°C for 2 h. The total pore volume of γ-Al_2O_3 is 1.08 cm^3 g^{-1} with surface area of 247 m^2 g^{-1} and the γ-Al_2O_3 granules were crushed into ~0.2 mm particles for use.

Catalyst characterizations

The x-ray diffraction (XRD) pattern was recorded on a Rigaku Uitima IV diffractometer with Cu Kα radiation (λ = 1.5418 Å, 35 kV, and 25 mA), and Scherrer equation was used to calculate the crystal size of NiO.

The specific surface area was calculated using the standard Brunauer–Emmett–Teller (BET) theory based on the N_2 adsorption isotherm obtained on a Belsorp max instrument (BEL, Japan) at −196°C. The pore-size distribution and total pore volume were determined using the Barrett–Joyner–Halenda (BJH) method.

The geometry and morphology of our Ni-Al_2O_3/Ni-foam composite catalyst was imaged by scanning electron microscopy (SEM, Hitachi S-4800; Japan) equipped with an energy dispersive x-ray (EDX) fluorescence spectrometer (Oxford; UK).

H_2 chemisorption was performed on a Quantachrome ChemBET 3000 chemisorption apparatus, 0.1 g sample was loaded into a quartz U-tube and heated from room temperature to 600°C at 10°C min^{-1} and maintained for 1 h under 10 vol % H_2/Ar flow, and then cooled down to 25°C in N_2. H_2 was introduced into the device to adsorb on the surface by pulse until saturated. The number of surface Ni sites per unit mass of catalyst was calculated by assuming the adsorption stoichiometry of H/Ni = 1:1.[49] H_2 temperature programmed surface reaction (H_2-TPSR) and temperature programmed reduction (H_2-TPR) were performed on a TP 5080 multifunctional automatic adsorption instrument (Xianquan Industrial and Trading Co., Ltd) with a thermal conductivity detector (TCD) and an online Mass Spectrometer (Proline Dycor, AMETEK Process Instrument). For H_2-TPSR and H_2-TPR, the sample was heated from room temperature to 300°C at 10°C min^{-1} and maintained for 0.5 h under 30 mL min^{-1} He flow. Then the sample was cooled to room temperature, followed by heating to 750°C at 10°C min^{-1} under a 10.0 vol % H_2/N_2 atmosphere with a gas flow of 30 mL min^{-1}.

The turnover frequencies (TOFs), defined as the ratio of product molecules per active site of catalyst and time, were calculated for both Ni-Al_2O_3/Ni-foam and Ni/Al_2O_3 (as a reference) catalysts. Here TOF is defined by

$$\mathrm{TOF} = \frac{\text{Product Molecules}}{\text{Active Sites}\times\text{Time}} = \frac{V_{CO_2,in}\times Y}{V_m\times S_{Ni}\times W} \quad (1)$$

where $V_{CO_2,in}$ is the volume flow rates of CO_2 at the inlet (L s^{-1}), Y is the yield of methane, V_m is the molar volume of gas (22.4 L mol^{-1}, assuming ideal behavior), S_{Ni} is defined as surface Ni atoms per gram catalyst (mol g^{-1}) which was

determined by H_2 chemisorption at 25°C, and W is the mass of the catalyst (g).

The composition of the catalyst sample was analyzed by a Thermo Scientific iCAP 6300 inductively coupled plasma atomic emission spectrometry (ICP-AES) on a United States Thermo IRIS Intrepid II XSP ICP spectrometer.

Catalyst test

The hydrogenation of CO_2 to methane was performed in a fixed-bed quartz tube reactor (600 mm length by 16 mm inner diameter) under atmospheric pressure. The catalyst dosage was 1.0 g if not specified. Prior to the reaction, the catalyst was prereduced in H_2 flow at 550°C for 2 h. A mixture of H_2/CO_2 (molar ratio of 4/1) was preheated to the desired temperature and then fed into the reactor continuously. The H_2 and CO_2 were all controlled by the calibrated mass flow controllers. The product effluent was analyzed using an online-gas chromatograph equipped with TCD and 2 m Shincarbon ST column (DIMKA). No coke was found on the catalyst during the reactivity tests. The CO_2 conversion (X) and methane selectivity (S) were calculated using standard normalization method on the base of carbon atom balance and defined as follows

$$X(\%) = \frac{V_{CO_2,in} - V_{CO_2,out}}{V_{CO_2,in}} \times 100 = \frac{A_{CO,out} \times f_{CO,out} + A_{CH_4,out} \times f_{CH_4,out}}{A_{CO_2,out} \times f_{CO_2,out} + A_{CO,out} \times f_{CO,out} + A_{CH_4,out} \times f_{CH_4,out}} \times 100 \quad (2)$$

$$S(\%) = \frac{V_{CH_4,out}}{V_{CO_2,in} - V_{CO_2,out}} \times 100 = \frac{A_{CH_4,out} \times f_{CH_4,out}}{A_{CO,out} \times f_{CO,out} + A_{CH_4,out} \times f_{CH_4,out}} \times 100 \quad (3)$$

where $V_{i,in}$ and $V_{i,out}$ are the volume flow rates of species i ($i = CO_2$ or CH_4) at the inlet and outlet (mL min^{-1}), $A_{j,out}$ and $f_{j,out}$ are the chromatographic peak area and the calibration factor of species j (j = CO, CO_2, or CH_4) at the outlet. Moreover, the $V_{CO_2,in}$ is assumed to be equal to the sum of $V_{CO_2,out}$, $V_{CH_4,out}$, and $V_{CO,out}$ because carbon deposition is ignorable.

Computational fluid dynamics calculation

The numerical simulation of the temperature distribution at steady state inside the fixed-bed quartz tubular reactor (i.d. = 16 mm) was based on the commercial Computational fluid dynamics (CFD) code FLUENT 6.3.26. All the simulations were carried out in a two-dimensional physical system. The tubular reactor was divided into three parts and the middle part in which catalyst placed was set isothermal. The catalytic bed contacting to the isothermal wall was initially at a uniform temperature of 320°C. In the simulation of hydrogenation of CO_2 to methane, 1.2 mL catalysts (Ni-Al_2O_3/Ni-foam, 0.75 g, void volume: 95 vol %; Ni/Al_2O_3, 0.95 g, void volume: 35 vol %) were packed in the reactors. The gas hourly space velocity (GHSV) was 10,000 h^{-1} and a mixture gas of CO_2 (40 mL min^{-1}) and H_2 (160 mL min^{-1}) was controlled by the calibrated mass flow controllers and fed into the reaction tube. According to the experiments, the CO_2 conversion was 82% and methane selectivity was 100%. The gas flow in the tube was laminar flow because the Reynolds number was smaller than 5 in this case. We assume that all the thermophysical properties of the materials (solids and gases) are functions of the local temperature and composition. The modeling and methods were given online in Supporting Information as well as other detailed information.

The kinetic experiment on activation energy (E_a) measurement under the kinetic-limiting region was performed and the data were obtained in an isothermal, tubular, one-pass differential, 6 mm inner diameter fixed-bed quartz reactor at ambient pressure. A mixture of H_2/CO_2 (molar ratio of 4/1) was preheated to the desired temperature and then passed through the catalyst bed. During the experiment, we kept the total flow gas and GHSV constant with different weights of the catalyst.[50]

Results and Discussion

Features of Ni-Al_2O_3/Ni-foam catalyst

Figures 1 and 2 show the textural/structural properties, reducibility, and morphology of our Ni-Al_2O_3/Ni-foam composite catalyst, indicating that the modified wet chemical etching is working efficiently and effectively for one-step creating and firmly embedding NiO-Al_2O_3 composite catalyst layer (~2 μm) into the Ni-foam struts. The specific surface area, mean NiO size, and numbers of the active Ni atoms on the catalyst surface were collected in Table 1 and Supporting Information Table S1. Figure 1a shows the N_2 adsorption–desorption isotherms of the fresh Ni-Al_2O_3/Ni-foam catalyst. This catalyst shows small amount of gas adsorbed at low relative pressure and provides a typical IV type isotherm according to the classification of International Union of Pure and Applied Chemistry (IUPAC) as evidenced by the appearance of a clear capillary condensation step in the P/P_0 region of 0.4–0.5. Moreover, the hysteresis loop with adsorption and desorption branches indicates a narrow BJH mesopore size distribution with an average pore diameter of 4–6 nm. As shown in Table 1, the specific surface area is increased from 3.9 m^2 g^{-1} of the neat Ni-foam to 26.3 m^2 g^{-1} of as-prepared catalyst (~7 times higher).

Figure 1b shows the XRD patterns of as-prepared catalyst before and after reduction. On the fresh catalyst, Bragg reflections of NiO phase is observed clearly at $2\theta = 37.4°$, 43.5°, and 63.2°, corresponding to (111), (200), and (220) planes of NiO crystals.[51,52] The estimated average size of the NiO particles is about 14.2 nm (as summarized in Table 1). No characteristic XRD peaks of Al_2O_3 can be observed indicating that the crystallites of Al_2O_3 are amorphous or highly dispersed.[53] After prereduction in H_2 at 550°C for 2 h, XRD patterns pattern of the NiO phase disappear, showing a good catalyst reducibility.

Figure 1c shows the H_2-TPR profile of the fresh catalyst, showing that the reduction of NiO starts from ~230°C and completely ends at ~600°C with three-peak feature. The first two TPR peaks at below 300°C are assignable to free small NiO particles while their weak signal intensity indicates a small amount of such NiO species. The strong TPR peak located in the range of 300–600°C is assignable to the reduction of dominant NiO particles (~14 nm, Table 1 and Figure 1b). Moreover, the NiO content in our foam-structured catalyst is estimated to be 12.6 wt %, according to the standard working curve of H_2-TPR peak area against NiO content (inset in Figure 1c).

Figure 2 presents the SEM images of the foam strut and the as-prepared Ni-Al_2O_3/Ni-foam catalyst. As shown in Figure 2a, the surface of untreated strut foam is smooth. After treated

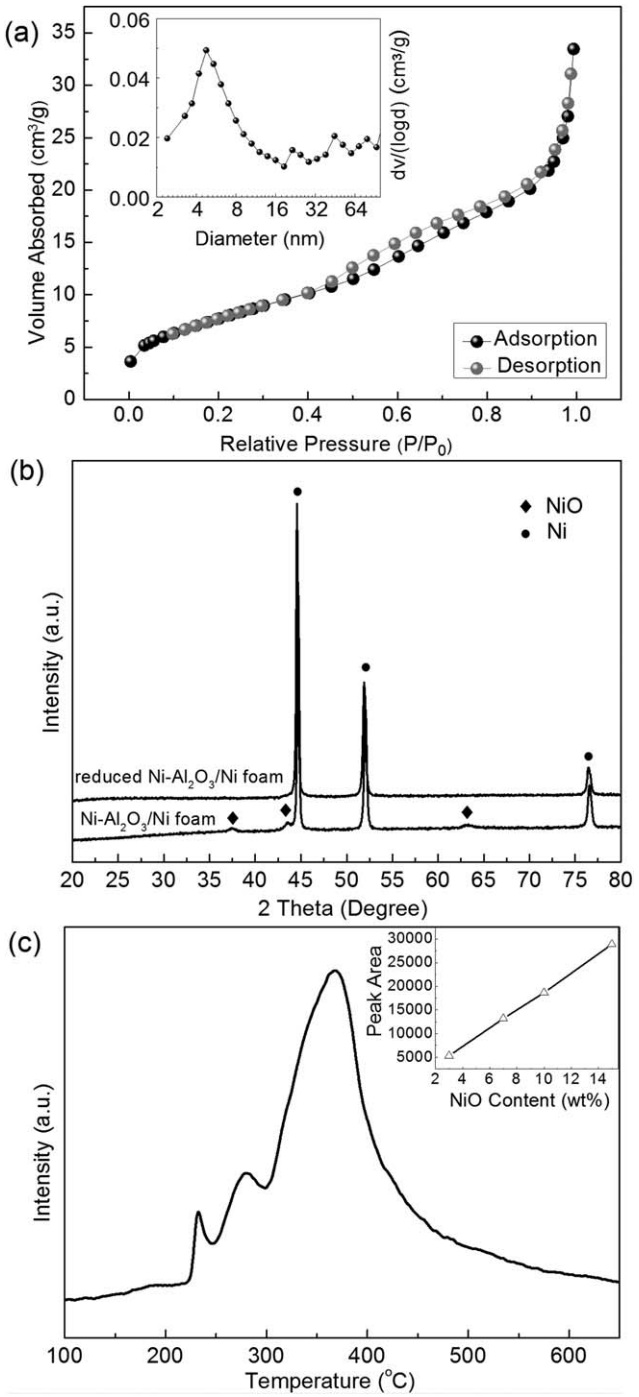

Figure 1. (a) N_2 adsorption-desorption isotherms and BJH mesopore size distribution (inset) of Ni-Al_2O_3/Ni-foam before reduction. (b) XRD patterns of as-prepared Ni-Al_2O_3/Ni-foam before and after reduction. (c) H_2-TPR profile of the Ni-Al_2O_3/Ni-foam and the standard working curve of H_2-TPR peak area against NiO content (inset).

by wet chemical etching and calcining, it is not surprising that the foam strut surface become coarse (Figure 2b), being covered with a very uniform porous layer ($\sim$2 μm in thickness) consisting of cubic-like nanocrystals (Figure 2c). As expected, such cubic-like nanocrystal coverage is composed of Al_2O_3 and NiO, being clearly evidenced by XRD patterns of NiO (Figure 1b) and EDX analysis (Supporting Information Figure S1). In addition, EDX results shows the cubic-like nanocrystal coverage with a composition of 77.2 wt % NiO and 22.8 wt % Al_2O_3 (NiO/Al_2O_3 mass ratio: $\sim$3.4) on the basis of O balance by excluding the bulk Ni-foam strut interference in the NiO quantification (Supporting Information Figure S1 and Text). Actually, NiO content is estimated to be 12.6 wt % of the whole catalyst by H_2-TPR (Figure 1c) while Al_2O_3 content is determined to be 4.2 wt % by means of ICP-AES. Accordingly, the NiO/Al_2O_3 mass ratio in the coverage layer is estimated to be 3.0 from the above H_2-TPR and ICP-AES results, which is in good agreement with the NiO/Al_2O_3 mass ratio of $\sim$3.4 from EDX analyses. After prereduced in H_2 at 550°C for 2 h, uniform Ni-Al_2O_3 nanocomposite particles (EDX element mapping, Supporting Information Figure S2) are formed and rooted separately on the foam strut surface (Figure 2d).

Catalyst performance

We initially checked the catalytic activity of our Ni-Al_2O_3/Ni-foam catalyst for the hydrogenation of CO_2 to methane, and compared with a common Ni/Al_2O_3 catalyst that is highly active and selective for the titled reaction.[49,54] Conversion, selectivity and TOF are collected also in the Table 1. Although the fresh Ni/Al_2O_3 catalyst possesses much higher specific surface area and smaller NiO crystal size than our Ni-Al_2O_3/Ni-foam catalyst, both reduced catalysts have almost equal surface nickel atom numbers (i.e., active sites). It is thus not surprising that both of them deliver comparable activity and selectivity. High conversion of 91% could be obtained for Ni-Al_2O_3/Ni-foam catalyst and 98% for Ni/Al_2O_3 while methane is the only hydrocarbon product at 300°C and a GHSV of 2500 h^{-1}. Moreover, both catalysts also provide very close TOF values, indicating almost equivalent intrinsic activity. As a control experiment, Ni-foams directly calcined in air at temperatures ranging from 300 to 600°C for 2 h were all prereduced in H_2 at 550°C for 2 h and tested in CO_2 methanation under identical reaction conditions, delivering the highest CO_2 conversion of only 10% with selectivity of >99.9%. The above results definitely indicate that the wet chemical etching method is very effective and efficient for not only creating highly active/selective Ni-based catalysts but also embedding them into the Ni-foam struts.

Figure 3 shows the temperature (reactor wall temperature) dependence of CO_2 methanation conversion and selectivity for both our Ni-Al_2O_3/Ni-foam and reference Ni/Al_2O_3 catalysts. Clearly, reaction could be lighted off over the foam-structured catalyst at $\sim$280°C and a sharp increase of CO_2 conversion from 32 to 91% is observed along with temperature up to 300°C. The CO_2 conversion reaches the highest value of 94% at 370°C and then declines continuously and smoothly down to 72% with further increasing temperature up to 550°C. The methane selectivity always remains at almost 100% at 240–400°C and then shows accelerating decline trend with further increasing temperature up to 550°C. Over the Ni/Al_2O_3 catalyst, similar evolution behavior is observed in the temperature dependence of CO_2 conversion and methane selectivity. Note that the Ni/Al_2O_3 shows a light-off temperature of $\sim$60°C lower than our Ni-Al_2O_3/Ni-foam catalyst while delivering higher CO_2 conversion at or below 300°C. This observation is most likely due to the big difference in their thermal conductivity, which causes great temperature contrast in catalyst bed (to see posterior part for detail). This also could be indirectly evidenced by their equivalent intrinsic activity expressed by TOFs; in TOF measurements, reaction heat effect has been

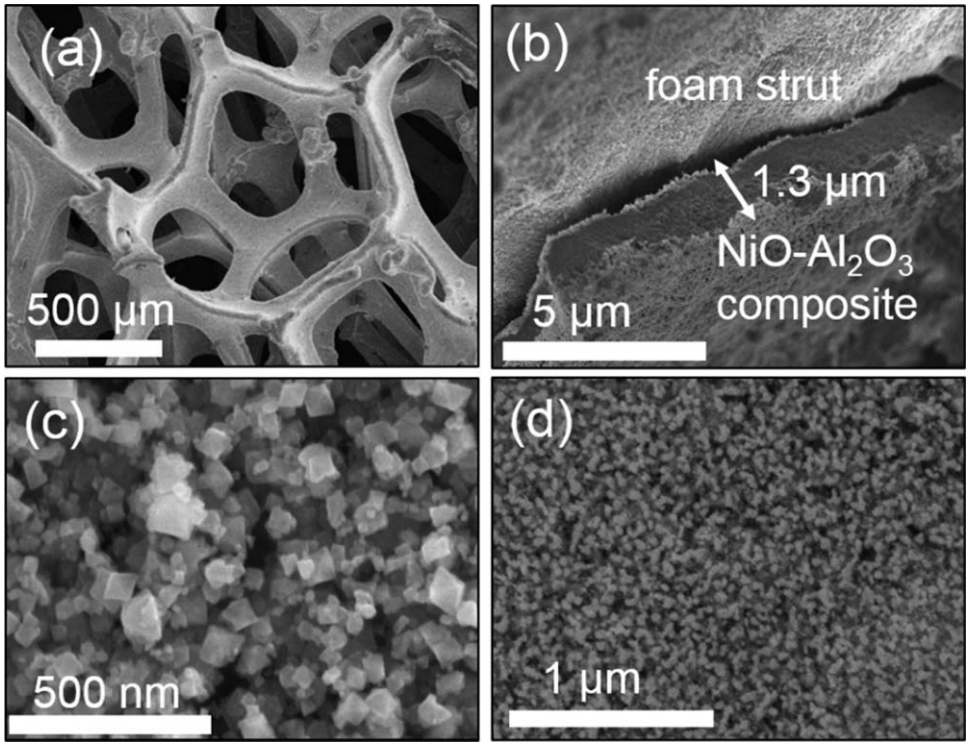

Figure 2. SEM images of (a) Nifoam, Ni-Al_2O_3/Ni-foam catalyst before (b, c), and after (d) reduction.

eliminated by controlling conversion to low level (e.g., <10%; Table 1 and Supporting Information Table S2). It is thus easy to understand why the CO_2 conversion reaches its maximum (thermodynamic equilibrium) at ~370°C for Ni-Al_2O_3/Ni-foam catalyst while ~290°C for the Ni/Al_2O_3. At high reactor wall temperature of >370°C, the CO_2 methanation moved in a region governed by partial external diffusion limitation at superficial gas velocity of < 2.79 cm s^{-1} (Supporting Information Figure S3), being consistent with the literature for the Ni-based catalysts in commercial SNG process.[21] This might neutralize the above observed difference in CO_2 conversion caused by different temperature rise of the two beds. As a result, the conversion and selectivity evolution curves for both catalysts are overlapped along with increasing temperature. Supporting Information Figure S4 shows the effect of GHSV on catalytic performance of the Ni-Al_2O_3/Ni-foam catalyst for CO_2 methanation. Clearly, in GHSV range studied from 2500 to 10,000 h^{-1}, at each temperature the CO_2 conversion declines with increase of GHSV as well as the methane selectivity.

Heat-transfer promotion

Our principle goal is to develop a catalyst with unique combination of excellent catalytic performance and excellent thermal conductivity that is essential to rapidly dissipate a large quantity of reaction heat released from such a strongly exothermic CO_2 methanation process. The above results clearly indicated that our foam-structured catalyst is highly active and selective for CO_2 methanation. We wonder whether such catalyst provided enhanced heat transfer, and if so, to what extent. To answer this question, the CFD simulation was used to illustrate the temperature distribution in our foam-structured catalyst bed as well as in the Ni/Al_2O_3 bed for comparison. For this effort, kinetic experiments on activation energy (E_a) measurement was performed under the kinetic-limiting region in an isothermal using the differential reactor.[50] Supporting Information Figure S5 shows the variation of the rate of reaction with temperature. An *E*a of ~85 kJ mol^{-1} is obtained on Ni-Al_2O_3/Ni-foam catalyst, being in well agreement with the literature results (39–89 kJ mol^{-1}) for the Ni-based catalysts (such as Ni/SiO_2).[55,56] This indicates that such foam-structured catalyst does not alter the nature of reaction, which is consistent with the fact of their equivalent intrinsic activity (TOFs in Table 1).

The CFD simulation modeling (Supporting Information Figure S6) and methods were established and given in the Supporting Information. For CFD calculation, the Ni-Al_2O_3/Ni-foam (void volume, 95%; Supporting Information Table S3)

Table 1. Physicochemical Characteristics and Catalytic Activity of Ni-Based Catalysts for the CO_2 Methanation

Catalyst	SSA[a] (m^2 g^{-1})	d_{NiO}[b] (nm)	Surf. Ni[c] (g^{-1})	X[d] (%)	S[d] (%)	TOF[e] (s^{-1})
Ni-Al_2O_3/Ni-foam	26/18	14.2	1.12×10^{20}	91	100	0.08
Ni/Al_2O_3	228/176	6.6	1.51×10^{20}	98	100	0.10

[a]Specific surface area (SSA) measured by N_2-BET method for fresh/reduced catalyst samples.
[b]NiO crystal size (d_{NiO}).
[c]Surface Ni atoms per gram catalyst, determined by H_2 chemisorption at 25°C assuming H/Ni ratio of 1.
[d]CO_2 conversion (X) and methane selectivity (S) for CO_2 hydrogenation at 300°C (0.1 MPa, $H_2/CO_2 = 4/1$, GHSV = 2500 h^{-1}).
[e]Turnover frequency to methane (expressed as: moles of methane formed per second per mole surface Ni atoms); CO_2 conversion is controlled to be <10% at 300°C for TOF calculation.

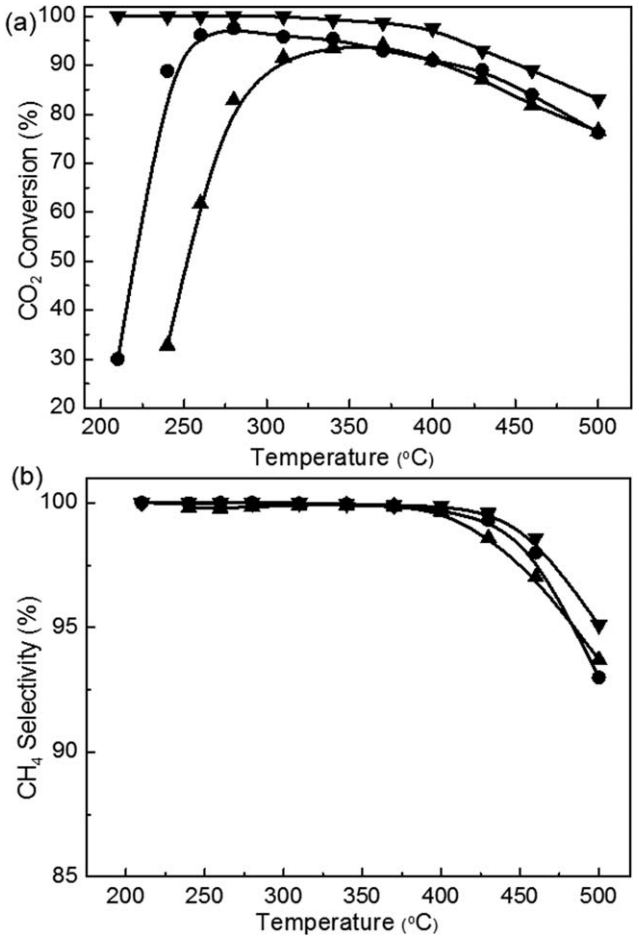

Figure 3. CO_2 conversion (a) and methane selectivity (b) for temperature-dependent hydrogenation of CO_2 over different catalysts: (▲) Ni-Al_2O_3/Ni-foam, (•) NiO/Al_2O_3, (▼) thermodynamic calculation.[54]

Reaction conditions: 1.0 g cat., 0.1 MPa, GHSV = 2500 h^{-1}, H_2/CO_2 (molar ratio) = 4/1.

and the reference catalyst of Ni/Al_2O_3 (0.2 mm, void volume, 35%; Supporting Information Table S3) were packed in the quartz tubular reactor (i.d., 16 mm) with catalyst dosage of 0.8 g. According to the experiments, the conversions of CO_2 in both beds are ~82% at 320°C for H_2/CO_2 (4/1) mixture feed gas flow rate of 200 mL min^{-1}. Figure 4 shows the steady-state temperature distribution within the two catalyst beds and the reaction rate along the axial direction in reaction beds is shown in Supporting Information Figure S6. In view of the strong exothermicity of CO_2 methanation process, a temperature rise of reaction bed is inevitable for both of the two catalysts. As clearly shown in Figure 4, the hot spot appears in the up-wind side of catalyst beds where the reaction takes place intensively as expected, which is in good agreement with the reaction rate along the axial direction (Supporting Information Figure S7). Whereas an equivalent amount of reaction heat is released from the catalyst surfaces at equal reactor conversion in both beds, our Ni-Al_2O_3/Ni-foam catalyst bed generates a hot spot with ~30°C temperature rise, being much smaller than that (~155°C) of Ni/Al_2O_3, due to the enhanced heat transfer of our foam-structured catalyst. Actually, as previously reported, the bed temperature rise of >300°C is observed inside pilot reactor with oxide-supported Ni catalyst for CO methanation.[14,20,21]

In addition, inside lab-scale reactor the temperature rises for both foam-structured and randomly PBs was also monitored by a thermal couple inserted inside with the results as shown in Figure 5. The structured bed of our Ni-Al_2O_3/Ni-foam catalyst delivers very small ΔT (temperature difference between the reactor wall temperature and the catalyst-bed temperature) of 18°C at 320°C (or 26°C at 400°C) at a high GHSV of 10,000 h^{-1}, being much lower than that of 125°C at 320°C (or 118°C at 400°C) in the Ni/Al_2O_3 PB. It is not surprising that reaction rate in the up-wind side of Ni-Al_2O_3/Ni-foam catalyst bed is much slower than the Ni/Al_2O_3 bed (Supporting Information Figure S7). Clearly, the CFD simulation results are well consistent with the experiment observation. Notably, the temperature rises inside both foam-structured and randomly PBs, by the CFD simulation at a reaction temperature of 320°C, are a little bit higher than the experimental observation by the thermal couple (30°C vs. 18°C for Ni-Al_2O_3/Ni-foam bed; 155°C vs. 125°C for Ni/Al_2O_3 bed). Such difference is likely attributed to two points: (1) thermal couple normally delivers an average temperature rather than hot-spot temperature and (2) model error caused by simplification of the real reaction system is unavoidably existed.

Stability

Besides high activity/selectivity and significantly enhanced heat transfer, our Ni-Al_2O_3/Ni-foam catalyst shows satisfying stability that is a very important practical consideration for a heterogeneous catalyst. A long-term test on this foam-

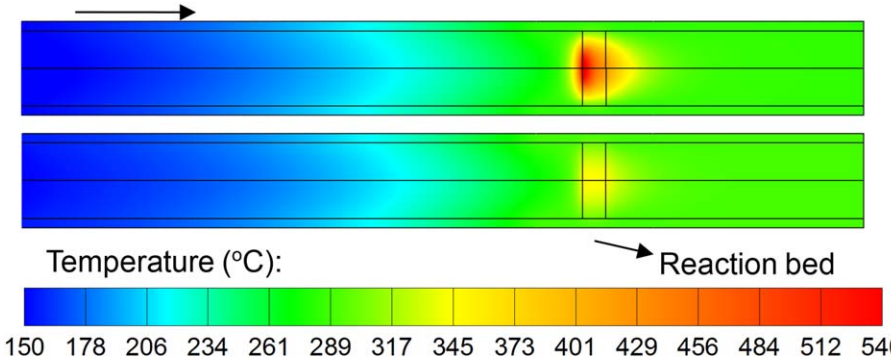

Figure 4. Temperature distribution at steady state inside reaction bed: Ni/Al_2O_3 (upper); Ni-Al_2O_3/Ni-foam catalyst (down).

[Color figure can be viewed in the online issue, which is available at wileyonlinelibrary.com.]

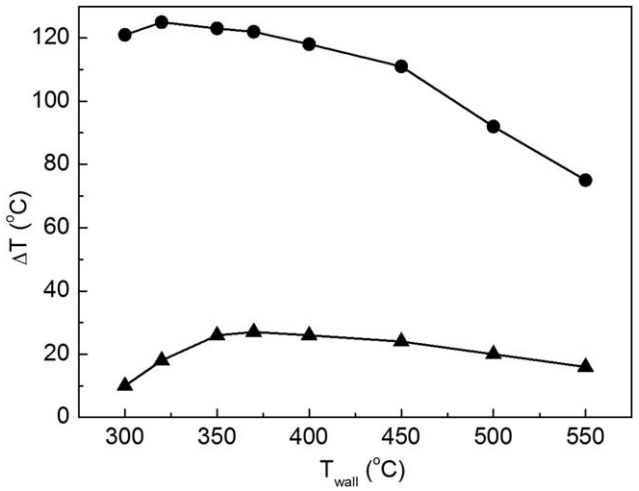

Figure 5. Temperature difference ($\triangle T$) between the reactor wall temperature (T_{wall}) and the catalyst-bed temperature (T_{bed}) over the catalysts of (▲) Ni-Al_2O_3/Ni-foam and (•) NiO/Al_2O_3, using a GHSV of 10,000 h^{-1}.

structured catalyst for the CO_2 methanation, with 10.2 mL catalyst packed into 16 mm inner diameter tubular reactor, was carried out at 320°C using a GHSV of 5000 h^{-1} with the results as shown in Figure 6. Considering such high catalyst dosage, the heat generated during the reaction would be enormous which may lead to a risk of high-temperature hop-spot generation in the bed and cause catalyst sintering and/or coking. By taking the advantage of significantly enhanced heat-transfer, the catalyst is superiorly stable with excellent activity (CO_2 conversion of ~90%) and CH_4 selectivity (>99.9%) maintenance throughout the entire 1200 h test. The used catalyst shows a little sintering, with surface morphology almost similar to that of the reduced catalyst (Figures 6b, c, used catalyst; Figure 2d, reduced catalyst). Its SSA thus is slightly reduced from ~18 to ~11 m^2 g^{-1} after undergoing 1200 h reaction. It should be pointed out that the SSA reduction occurred mainly at the beginning of the reaction, as we observe a SSA reduction from ~18 to 13 m^2 g^{-1} within only 100 h running. To avoid the illusion of the long lifetime caused by the excess of catalyst, another long-term test of our Ni-Al_2O_3/Ni-foam was carried out under the conditions far away from equilibrium with the results as shown in Supporting Information Figure S8. Using a high GHSV of 15,000 h^{-1}, CO_2 conversion was reduced to ~76% and subsequently demonstrated excellent maintenance with CH_4 selectivity always higher than 99.8% throughout the entire 500 h test at 320°C.

As well known, CH_4 pyrolysis to form carbon deposit will be favorable at high temperature (e.g., >557°C). In a pilot test for CO methanation with an inlet temperature of 300°C, oxide-supported Ni catalyst bed temperature can reach 675°C because of the poor heat transfer.[20,21] So, if the real bed temperature can be reduced lower than 600°C by improving the bed heat transfer, coking by CH_4 product pyrolysis would be significantly suppressed. In our case of 1200 h stability test, the real bed temperature is retained at 355 ±10°C monitored by a thermal couple inserted inside the reactor, due to the enhanced heat transfer ability of our Ni-foam-structured catalyst design. As a result, neither whisker carbon by SEM observation (Figures 6b, c) nor graphite carbon phase by XRD detection (Supporting Information Figure S9) could be detectable on the catalyst after 1200 h on stream. Only trace methane formation is detected on such used catalyst by an on-line mass spectrometry in H_2 temperature programmed surface reaction (TPSR, Supporting Information Figure S10), being assignable to hydrogenation gasification of surface active carbon intermediates such as surface NiC_x.[55,57,58]

Furthermore, we extend the application of Ni-Al_2O_3/Ni-foam catalyst in the CO methanation ($\Delta H_{25°C} = -206$ kJ mol^{-1}) that is more strongly exothermic than CO_2 methanation ($\Delta H_{25°C} = -165$ kJ mol^{-1}), aiming to verify the feasibility of our foam-structured Ni-based catalyst for the production of SNG from syngas through methanation of both CO and

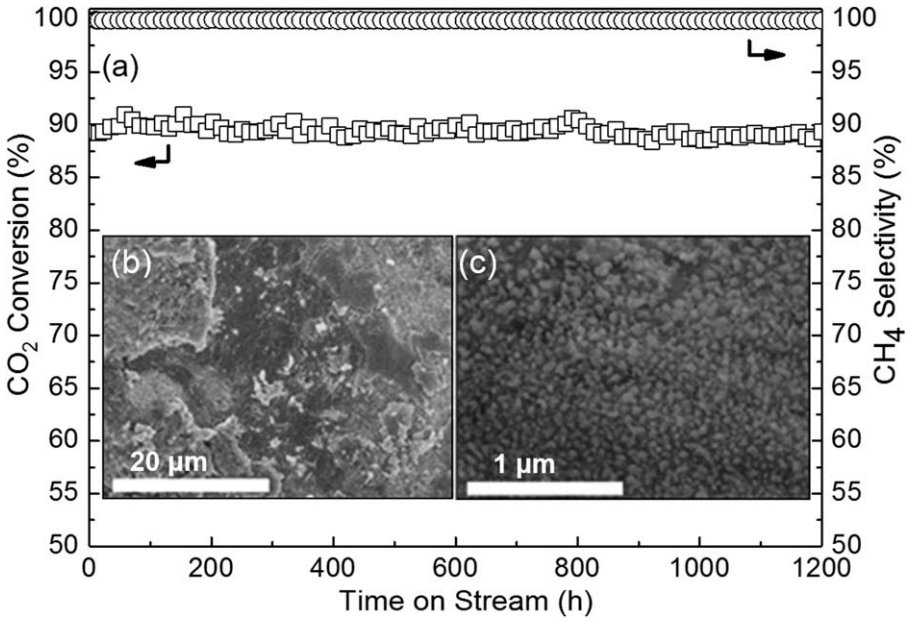

Figure 6. (a) CO_2 conversion and methane selectivity for CO_2 methanation vs. time on stream using Ni-Al_2O_3/Ni-foam catalyst (10.2 mL catalyst, $H_2/CO_2 = 4/1$, GHSV = 5000 h^{-1}, 320°C).

SEM images from low magnitude (b) to high magnitude (c) of the catalysts after 1200 h test.

CO_2. Most interestingly, this catalyst is also working efficiently in CO methanation, delivering a CO conversion of >99% and a CH_4 selectivity of 93% for a feed of H_2/CO (3/1) at 330°C and 0.1 MPa with a GHSV of 5000 h^{-1} and showing excellent activity/selectivity maintenance throughout a 500 h test in a PB with 10.4 mL our foam-structured catalyst (Supporting Information Figure S11). We anticipate that our approach opens a new opportunity for development of an energy-efficient SNG process, due to the enhanced heat transfer that would permit to avoid cascades of reactors and recycles for reaction heat moving away as it is the case in actual process.

Conclusions

We report a novel foam-structured Ni-Al_2O_3 catalyst for the strongly exothermic CO_2 methanation reaction. This catalyst is obtainable by facile modified wet chemical etching method, demonstrating a combination of high activity/selectivity, high stability, and significantly enhanced heat transfer. Uniform NiO-Al_2O_3 composite catalyst layer ($\sim$2 μm) is efficiently formed and firmly anchored onto the foam struts by directly immersing the Ni-foam substrate into a chemical etching solution consisting of SDS, acetic acid, and aluminum nitrate for 2 h at 65°C, followed by a calcination in air. High CO_2 conversion of $\sim$90% and very high methane selectivity of >99.9% can be obtained and maintained for a feed of H_2/CO_2 (4/1) at 320°C and 0.1 MPa with a GHSV of 5000 h^{-1}, throughout entire 1200 h test in a PB with 10.2 mL our foam-structured catalyst. CFD calculation and experimental measurement consistently show a big reduction of "hotspot" temperature due to highly enhanced heat transfer.

Acknowledgments

This work was financially supported by the "973 program" (2011CB201403) from the MOST of China, and the NSF of China (21473057, 21273075, and U1462129).

Literature Cited

1. Olah GA, Prakash GKS, Goeppert A. Anthropogenic chemical carbon cycle for a sustainable future. *J Am Chem Soc*. 2011;133:12881–12898.
2. Federsel C, Jackstell R, Beller M. State-of-the-art catalysts for hydrogenation of carbon dioxide. *Angew Chem Int Ed*. 2010;49:6254–6257.
3. Wang W, Wang SP, Ma XB, Gong JL. Recent advances in catalytic hydrogenation of carbon dioxide. *Chem Soc Rev*. 2011;40:3703–3727.
4. He MY, Sun YH, Han BX, Green carbon science: scientific basis for integrating carbon resource processing, utilization, *and recycling*. *Angew Chem Int Ed*. 2013;52:9620–9633.
5. Graciani J, Mudiyanselage K, Xu F, Baber AE, Evans J, Senanayake SD, Stacchiola DJ, Liu P, Hrbek J, Sanz JF, Rodriguez JA. Highly active copper-ceria and copper-ceria-titania catalysts for methanol synthesis from CO_2. *Science*. 2014;345(6196):546–550.
6. Schuchmann K, Müller V. Direct and reversible hydrogenation of CO_2 to formate by a bacterial carbon dioxide reductase. *Science*. 2013;342:1382–1385.
7. Kondratenko EV, Mul G, Baltrusaitis J, Larrazábal GO, Pérez-Ramírez J. Status and perspectives of CO_2 conversion into fuels and chemicals by catalytic, photocatalytic and electrocatalytic processes. *Energy Environ Sci*. 2013;6:3112–3135.
8. Wu TS, Zou LY, Han DX, Li FH, Zhang QX, Niu L. A carbon-based photocatalyst efficiently converts CO_2 to CH_4 and C_2H_2 under visible light. *Green Chem*. 2014;16:2142–2146.
9. Benson EE, Kubiak CP, Sathrum AJ, Smieja JM. Electrocatalytic and homogeneous approaches to conversion of CO_2 to liquid fuels. *Chem Soc Rev*. 2009;38:89–99.
10. Kuhl KP, Cave ER, Abram DN, Jaramillo TF. New insights into the electrochemical reduction of carbon dioxide on metallic copper surfaces. *Energy Environ Sci*. 2012;5:7050–7059.
11. Reske R, Mistry H, Behafarid F, Cuenya BR, Strasser P. Particle size effects in the catalytic electroreduction of CO_2 on Cu nanoparticles. *J Am Chem Soc*. 2014;136:6978–6986.
12. Centi G, Quadrelli EA, Perathoner S. Catalysis for CO_2 conversion: a key technology for rapid introduction of renewable energy in the value chain of chemical industries. *Energy Environ Sci*. 2013;6:1711–1731.
13. Wang W, Chen J, Li C, Tian W. Achieving solar overall water splitting with hybrid photosystems of photosystem II and artificial photocatalysts. *Nat Commun*. 2014;5:4647.
14. Kopyscinski J, Schildhauer TJ, Biollaz SMA. Production of synthetic natural gas (SNG) from coal and dry biomass—a technology review from 1950 to 2009. *Fuel*. 2010;89:1763–1783.
15. Li DS. Competition analysis for coal based synthetic natural gas. *Coal Chem Ind*. 2007;133:1–3.
16. Du GA, Lim SY, Yang YH, Wang C, Pfefferle L, Haller GL. Methanation of carbon dioxide on Ni-incorporated MCM-41 catalysts: the influence of catalyst pretreatment and study of steady-state reaction. *J Catal*. 2007;249:370–379.
17. Weatherbee GD, Bartholomew CH. Hydrogenation of CO_2 on group VIII metals: IV. Specific activities and selectivities of silica-supported Co, Fe, and Ru. *J Catal*. 1984;87:352–362.
18. Abe T, Tanizawa M, Watanabe K, Taguchi A. CO_2 methanation property of Ru nanoparticle-loaded TiO_2 prepared by a polygonal barrel-sputtering method. *Energy Environ Sci*. 2009;2:315–321.
19. Karelovic A, Ruiz P. Improving the hydrogenation function of Pd/γ-Al_2O_3 catalyst by Rh/γ-Al_2O_3 addition in CO_2 methanation at low temperature. *ACS Catal*. 2013;3:2799–2812.
20. Rostrup-Nielsen JR, Pedersen K, Sehested J. High temperature methanation sintering and structure sensitivity. *Appl Catal A*. 2007;330:134–138.
21. Nguyen TTM, Wissing L, Skjøth-Rasmussen MS. High temperature methanation: Catalyst considerations. *Catal Today*. 2013;215:233–238.
22. Werther J. Fluidized-bed reactors. In: Ertl G, Knozinger H, Schuth F, Weitkamp J, editors. *Handbook of Heterogeneous Catalysis, 2nd ed*. Weinheim: Wiley-VCH, 2008:2106–2132.
23. Tappan BC, Huynh MH, Hiskey MA, Chavez DE, Luther EP, Mang JT, Son SF. Ultralow-density nanostructured metal foams: combustion synthesis, morphology, and composition. *J Am Chem Soc*. 2006;128:6589–6594.
24. Dautzenberg FM. New catalyst synthesis and multifunctional reactor concepts for emerging technologies in the process industry. *Catal Rev*. 2004;46:335–368.
25. Renken A, Kiwi-Minsker L. Microstructured catalytic reactors. *Adv Catal*. 2010;53:47–122.
26. Chen W, Zhao GF, Xue QS, Chen L, Lu Y. High carbon-resistance Ni/$CeAlO_3$-Al_2O_3 catalyst for CH_4/CO_2 reforming. *Appl Catal B*. 2013;136–137:260–268.
27. Chen W, Sheng WQ, Zhao GF, Cao FH, Xue QS, Chen L, Lu Y. Microfibrous entrapment of Ni/Al_2O_3 for dry reforming of methane: a demonstration on enhancement of carbon resistance and conversion. *RSC Adv*. 2012;2:3651–3653.
28. Sheng M, Yang HY, Cahela DR, Tatarchuk BJ. Novel catalyst structures with enhanced heat transfer characteristics. *J Catal*. 2011;281:254–262.
29. Sheng M, Yang HY, Cahela DR, Yantz WR Jr., Gonzalez CF, Tatarchuk BJ. High conductivity catalyst structures for applications in exothermic reactions. *Appl Catal A*. 2012;445–446:143–152.
30. Wang XY, Wen M, Wang CZ, Ding J, Sun Y, Liu Y, Lu Y. Microstructured fiber@HZSM-5 core-shell catalysts with dramatic selectivity and stability improvement for the methanol-to-propylene process. *Chem Commun*. 2014;50:6343–6345.
31. Wen M, Wang XY, Han LP, Ding J, Sun Y, Liu Y, Lu Y. Monolithic metal-fiber@HZSM-5 core-shell catalysts for methanol-to-propylene. *Microporous Mesoporous Mater*. 2015;206:8–16.
32. Zhang QF, Li YK, Zhang L, Chen L, Liu Y, Lu Y. Structured nanoporous-gold/Al-fiber: galvanic deposition preparation and reactivity for the oxidative coupling of methanol to methyl formate. *Green Chem*. 2014;16:2992–2996.
33. Zhang QF, Li YK, Zhang L, Chen L, Liu Y, Lu Y. Thin-sheet microfibrous-structured nanoporous gold/Al fiber catalysts for oxidative coupling of methanol to methyl formate. *J Catal*. 2014;317:54–61.

34. Zhao GF, Hu HY, Deng MM, Lu Y. Microstructured Au/Ni-fiber catalyst for low-temperature gas-phase selective oxidation of alcohols. *Chem Commun*. 2011;47:9642–9644.
35. Zhao GF, Deng MM, Jiang YF, Hu HY, Huang J, Lu Y. Microstructured Au/Ni-fiber catalyst: galvanic reaction preparation and catalytic performance for low-temperature gas-phase alcohol oxidation. *J Catal*. 2013;301:46–53.
36. Zhao GF, Hu HY, Deng MM, Ling M, Lu Y. Au/Cu-fiber catalyst with enhanced low-temperature activity and heat transfer for the gas-phase oxidation of alcohols. *Green Chem*. 2011;13:55–58.
37. Zhao GF, Li YK, Zhang QF, Deng MM, Cao FH, Lu Y. Galvanic deposition of silver on 80-μm-Cu-fiber for gas-phase oxidation of alcohols. *AIChE J*. 2014;60:1045–1053.
38. Giani L, Groppi G, Tronconi E. Mass-transfer characterization of metallic foams as supports for structured catalysts. *Ind Eng Chem Res*. 2005;44:4993–5002.
39. Gascon J, van Ommen JR, Moulijn JA, Kapteijn F. Structuring catalyst and reactor—an inviting avenue to process intensification. *Catal Sci Technol*. 2015;5:807–817.
40. Giani L, Cristiani C, Groppi G, Tronconi E. Washcoating method for Pd/γ-Al_2O_3 deposition on metallic foams. *Appl Catal B*. 2006;62:121–131.
41. Montebelli A, Visconti CG, Groppi G, Tronconi E, Cristiani C, Ferreira C, Kohler S. Methods for the catalytic activation of metallic structured substrates. *Catal Sci Technol*. 2014;4:2846–2870.
42. Sirijaruphan A, Goodwin JG Jr., Rice RW, Wei DG, Butcher KR, Roberts GW, Spivey JJ. Metal foam supported Pt catalysts for the selective oxidation of CO in hydrogen *Appl Catal A*. 2005;281:1–9.
43. Qian BT, Shen ZQ. Fabrication of superhydrophobic surfaces by dislocation-selective chemical etching on aluminum, copper, and zinc substrates. *Langmuir*. 2005;21:9007–9009.
44. Li LN, Dong HR, Bi PY, Preparation of aluminum superhydrophobic surface with nano-micro mixed structure by SDBS/HCl etching method. *Chem J Chin Univ*. 2009;30:1371–1374.
45. Liu Y, Wang H, Li JF, Lu Y, Wu HH, Xue QS, Chen L. Monolithic microfibrous nickel catalyst co-modified with ceria and alumina for miniature hydrogen production via ammonia decomposition. *Appl Catal A*. 2007;328:77–82.
46. Xiong J, Dong XF, Song YB, Dong YC. A high performance Ru-ZrO_2/carbon nanotubes-Ni foam composite catalyst for selective CO methanation. *J Power Sources*. 2013;242:132–136.
47. Cai SX, Zhang DS, Shi LY, Xu J, Zhang L, Huang L, Li HR, Zhang JP. Porous Ni-Mn oxide nanosheets in-situ formed on nickel foam as 3D hierarchical monolith de-NO_x catalysts. *Nanoscale*. 2014;6:7346–7353.
48. Peng PY, Jin I, Yang TCK, Huang CM. Facile preparation of hierarchical CuO-CeO_2/Ni metal foam composite for preferential oxidation of CO in hydrogen-rich gas. *Chem Eng J*. 2014;251:228–235.
49. Gao JJ, Jia CM, Zhang MJ, Gu FN, Xu GW, Su FB. Effect of nickel nanoparticle size in Ni/α-Al_2O_3 on CO methanation reaction for the production of synthetic natural gas. *Catal Sci Technol*. 2013;3:2009–2015.
50. Shinde VM, Madras G. CO methanation toward the production of synthetic natural gas over highly active Ni/TiO_2 catalyst. *AIChE J*. 2014;60:1027–1035.
51. Ocampo F, Louis B, Roger AC. Methanation of carbon dioxide over nickel-based $Ce_{0.72}Zr_{0.28}O_2$ mixed oxide catalysts prepared by sol-gel method. *Appl Catal A*. 2009:369;90–96.
52. Hu DC, Gao JJ, Ping Y, Jia LH, Gunawan P, Zhong ZY, Xu GW, Gu FN, Su FB. Enhanced investigation of CO methanation over Ni/Al_2O_3 catalysts for synthetic natural gas production. *Ind Eng Chem Res*. 2012;51:4875–4886.
53. Galvis HMT, Bitter JH, Khare CB, Ruitenbeek M, Dugulan AI, de Jong KP. Supported iron nanoparticles as catalysts for sustainable production of lower olefins. *Science*. 2012;335:835–838.
54. Garbarino G, Riani P, Magistri L, Busca G. A study of the methanation of carbon dioxide on Ni/Al_2O_3 catalysts at atmospheric pressure. *Int J Hydrogen Energy*. 2014;39:11557–11565.
55. Weatherbee GD, Bartholomew CH. Hydrogenation of CO_2 on group VIII metals: II. Kinetics and mechanism of CO_2 hydrogenation on nickel. *J Catal*. 1982;77:460–472.
56. Weatherbee GD, Bartholomew CH. Hydrogenation of CO_2 on group VIII metals: I. Specific activity of Ni/SiO_2. *J Catal*. 1981;68:67–76.
57. Akamaru S, Shimazaki T, Kubo M, Abe T. Density functional theory analysis of methanation reaction of CO_2 on Ru nanoparticle supported on TiO_2 (101). *Appl Catal A*. 2014;470:405–411.
58. Bartholomew CH, Pannell RB. The stoichiometry of hydrogen and carbon monoxide chemisorption on alumina- and silica-supported nickel. *J Catal*. 1980;65:390–401.

Manuscript received Mar. 26, 2015, and revision received May 22, 2015.